OTREC, PREDICT and EC model to study convection

Zeljka Fuchs-Stone[1], Stipo Sentic[2], David J. Raymond[1], and Peter Bechtold[3]

[1]New Mexico Tech
[2]New Mexico Institute of Mining and Technology
[3]European Center for Medium range Weather Forecast, UK

November 23, 2022

Abstract

Two data sets (OTREC and PREDICT) and the European Center operational model are used to study convection.

Vertically integrated moisture convergence is taken to be a proxy for convection. The interplay between the thermodynamic parameters is examined for weak and strong convection. It is found that for strong convection saturation fraction anti-correlates with instability index and DCIN in a similar manner for all analyzed regions of PREDICT and OTREC.

The European Center model is used to look at the composite diurnal cycles of strong and weak convection. As convection increases, saturation fraction increases while instability index and DCIN decrease as in OTREC and PREDICT. The boundary layer and free troposphere thus both play an important role in convection development.

OTREC, PREDICT and EC model to study convection

Ž. Fuchs-Stone[1,2], S. Sentić[1], D. J. Raymond[1,2], and P. Bechtold[3]

[1]Climate and Water Consortium, New Mexico Tech, 801 Leroy Place, Socorro, NM.

[2]Physics Department, New Mexico Tech, 801 Leroy Place, Socorro, NM.

[3]European Centre for Medium-Range Weather Forecasts, Shinfield Park, Reading, United Kingdom

Corresponding author: Željka Fuchs-Stone (zeljka.fuchs@nmt.edu)

Key points:

- Both boundary layer and free tropospheric characteristics are important for development of convection.
- Field project and modeling data agree on the interplay of thermodynamic parameters.

Abstract

Two data sets (OTREC and PREDICT) and the European Center operational model are used to study convection.

Vertically integrated moisture convergence is taken to be a proxy for convection. The interplay between the thermodynamic parameters is examined for weak and strong convection. It is found that for strong convection saturation fraction anti-correlates with instability index and DCIN in a similar manner for all analyzed regions of PREDICT and OTREC.

The European Center model is used to look at the composite diurnal cycles of strong and weak convection. As convection increases, saturation fraction increases while instability index and DCIN decrease as in OTREC and PREDICT. The boundary layer and free troposphere thus both play an important role in convection development.

Plain Language Summary

Convection in the tropics is the main mechanism that brings bad weather, storms and hurricanes there. Understanding how convection develops and what it depends on is a question that we have been trying to answer for many decades. The characteristics of the environment can help in this task. The data from two field projects, OTREC and PREDICT, as well as from the European Center model are analyzed here to show what characteristics of the environment are important for convection. This can help us in improving the weather models and forecasts that are very much needed in the tropics.

1. Introduction

Mesoscale convective systems (MCS) are responsible for most rain in the tropics (Houze, 1989). They are ensembles of convection that are often idealized as entraining plumes of 1 - 5 km diameter that go through their life cycle almost independently of one another. If the convection grows in time that implies that the number of plumes is getting larger and convection covers a larger area, while when convection decays, their number is getting smaller (Arakawa and Shubert 1974; Zipser, 1969, 1977; Houze, 1989, 2004; etc.; Ed Zipser, personal communication).

Another school of thought tries to study the broader properties of MCSs and most importantly their interaction with the environment (Raymond et al., 2011). This approach does not look at the internal structure of the MCSs, but how the environment governs their overall characteristics. The goal is to identify the thermodynamic properties of the environment that govern MCSs. If one gets those right, it would be possible to correctly parametrize convection (Raymond and Fuchs-Stone, 2020).

What properties of the environment guide MCSs? Is it the boundary layer, the free troposphere or both? There are many papers that suggest that the boundary layer is responsible for the intertropical convergence zone, ITCZ (Riehl et al., 1951; Lindzen and Nigam, 1987; Battisti et al., 1999; Tomas et al., 1999; Stevens et al., 2002). Back and Bretherton (2009) postulate two types of convection, one that is generated by the boundary layer convergence and another that is generated by the free troposphere noting that the boundary layer convergence is of more importance in east and central

55 Pacific ITCZ. Raymond (2017) advocates for the importance of thermodynamic factors in this
56 region, mainly in the free troposphere.

57 Based on Fuchs-Stone et al. (2020) and Raymond and Fuchs (2020), we hypothesize that saturation
58 fraction, instability index and DCIN play an important role in development of convection.

59 The saturation fraction is defined as precipitable water divided by the saturated precipitable water
60 and it is a measure for column relative humidity.

61 The instability index is defined as the difference between the saturated moist entropies averaged
62 over the altitude ranges of 1-3 km and 5-7 km. The instability index is a measure of low to mid-
63 tropospheric moist convective instability. Lower, but still positive, values are associated with
64 higher saturation fraction and more rainfall (Raymond et al., 2014, Gjorgjievska and Raymond,
65 2014, Raymond et al., 2015, Sentic et al., 2015, Raymond and Flores, 2016, Singh et al., 2019,
66 Raymond and Kilroy, 2019). We call this association "moisture quasi-equilibrium".

67 Deep convective inhibition (DCIN) is defined as the difference between the average of the
68 saturated moist entropy in the 1.5 - 2 km layer and the boundary layer moist entropy averaged over
69 the 0 - 1 km layer.

70 In this paper we choose vertically integrated moisture convergence, represented in energy terms,
71 to be to be a proxy for convection. It is defined as:

72 $$\mathrm{MC} = -L \int \nabla \cdot (\rho \boldsymbol{v} r)$$

73 where ρ is the density, $\boldsymbol{v}$ is the horizontal velocity, r is the mixing ratio and L is the latent heat of
74 condensation. It should be noted that there are other degrees of freedom that might be active in
75 determining what governs convection. We choose vertically integrated moisture convergence
76 because it is a good parameter when estimating rainfall. Based on moisture convergence, we
77 classify convection into strong and weak categories. We then look at the interplay between the
78 thermodynamic parameters and convection.

79 We use the dropsonde data sets from two field projects: OTREC (Organization of Tropical East
80 Pacific Convection) which took place in 2019 and PREDICT (Pre-Depression Investigation of
81 Cloud-Systems in the Tropics) which took place in 2010.

82 OTREC studied all phases of convection over the East Pacific and Southwest Caribbean from
83 Liberia, Costa Rica using the NSF/NCAR Gulfstream V aircraft (Fuchs-Stone et al., 2020).
84 Twenty-two research missions were flown and 648 dropsondes were successfully deployed in a
85 grid of three regions of diverse environments. The research flight area in the Eastern Pacific ITCZ,
86 B2, covers the region with strong meridional sea surface temperature (SST) gradients, while B1b,
87 the Caribbean region, covers the area with uniform and moderately high SSTs. The B1a box is
88 located just off the Pacific coast of Colombia and it covers the environment of lower SSTs in the
89 proximity of land.

90 PREDICT studied systems with potential to develop into tropical cyclones in the Western Atlantic
91 and Caribbean using the NSF/NCAR Gulfstream V aircraft (Montgomery et al., 2012). Twenty-
92 six research missions were flown and 547 drospondes were deployed. The PREDICT data covers
93 a vast region with high SSTs and higher latitudes than OTREC.

94

Three-dimensional variational analysis (3DVAR) of dropsonde data is performed to obtain regular grids of data 0.5 by 0.5 degree for OTREC and 1 by 1 degree for PREDICT (Lopez and Raymond, 2011; Raymond and Lopez, 2011; Raymond et al., 2011; Montgomery et al., 2012; Gjorgjievska and Raymond, 2014; Juracic and Raymond, 2016; Fuchs-Stone et al., 2020; Raymond and Fuchs-Stone, 2020). The data set for dropsondes used in this paper is NCAR/EOL AVAPS Dropsonde Quality Controlled Data Version 1.0, Voemel, H. (2019). The grids for OTREC and PREDICT are different to avoid sample size artifact.

Finally, we look at the time evolution, i.e. composite diurnal cycle of the thermodynamic parameters in strong and weak convection using the operational European Centre for Medium-Range Weather Forecasts (ECMWF) model.

Section 2 presents the results and their interpretation, while conclusions are given in section 3.

2. Results

2.1 The interplay between convection and thermodynamic parameters

Figure 1 shows how our thermodynamic parameters saturation fraction, instability index and DCIN correlate with moisture convergence, i.e. convection. Each dot for OTREC data set represents the average in half a degree by half a degree box obtained from the 3DVAR, one by one degree average for PREDICT data. PREDICT data is shown in green, the data for the Eastern Pacific ITCZ box B2 in blue, the Pacific box off the coast of Colombia, B1a, is shown in red and the data for the Caribbean B1b box is shown in black. We see that higher values of saturation fraction lead to more convection. The opposite is true for the instability index where lower values correspond to more convection. Negative and small positive values of DCIN lead to more convection as well (Raymond et al., 2003).
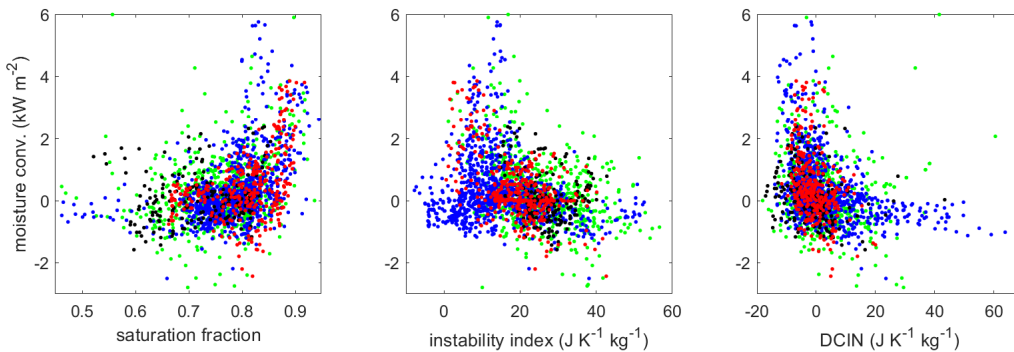

Figure 1: Scatter plot of moisture convergence and saturation fraction, instability index and DCIN. Green dots are PREDICT data, blue Eastern Pacific ITCZ, red Colombian box and black Caribbean box.

To decipher Figure 1, that includes all cases from null to strong convection, we now set out to look at the relationships between our thermodynamic parameters saturation fraction, instability index and DCIN for strong and weak convection. We define convection by the strength of vertically

125 integrated moisture convergence. If moisture convergence is greater than 2 kWm^{-2} we define it
126 as strong convection and if it is less than 0.5 kWm^{-2} we define it as weak convection.

127
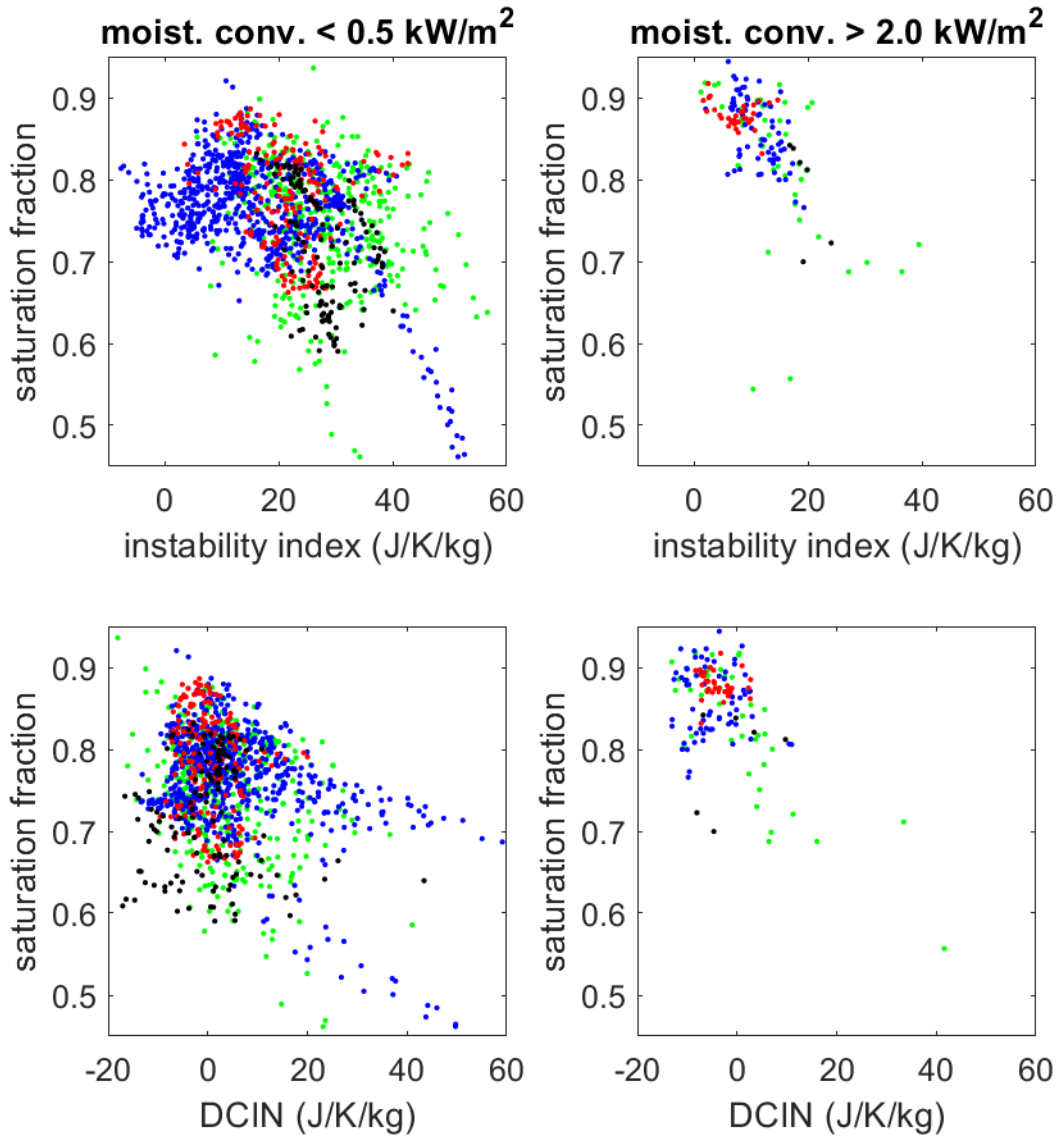
Figure 2: Scatter plots between saturation fraction and instability index (top panel) and saturation
fraction and DCIN (bottom panel) for weak convection (left) and strong convection (right).

130 Figure 2 shows scatter plots between saturation fraction and instability index and saturation
131 fraction and DCIN for strong convection and weak convection for PREDICT and OTREC data.
132 For strong convective cases the saturation fraction and instability index show a clear anti-
133 correlation as per moisture quasi-equilibrium theory. The scatter plot between saturation fraction
134 and DCIN shows that negative or very small DCIN is required for strong convection. The scatter
135 plot for weak convection is significantly more scattered (including some outliers in B2 and
136 PREDICT regions). The saturation fraction can be lower than expected in this case. This is because

137   the environment in weak convection is too dry and moisture quasi-equilibrium theory does not
138   hold. DCIN turns towards higher positive values.

139   Figures 1 – 2 tell an interesting story. Strong convection seems to be similar in all regions
140   irrespective of sea surface temperature (SST) (high in PREDICT, lower in B1b and even lower in
141   B2 and B1a), whether we are close to land (B1a box) or not. Once there is significant convection,
142   there is no doubt that moisture convergence depends on high saturation fraction, low instability
143   index and low DCIN. Furthermore, saturation fraction anti-correlates with instability index and
144   DCIN in a similar manner. When convection is weak and the environment is dry, the time scale
145   for convection to adjust the moisture to the equilibrium value for a given value of instability index
146   is long and this anti-correlation is not necessarily observed. DCIN takes up higher values indicating
147   inversion.

148   **2.2 Composite diurnal cycle**

149   To look at the time evolution of convection for OTREC we look at the composite diurnal cycles
150   from the operational EC model for days with OTREC observations. We first use the 3DVAR
151   moisture convergence data to define strong convective and weak convective cases. We then
152   average the ECMWF operational model data in boxes with the same longitude and latitude for all
153   times of the same day. Then we average all the hourly values. The same method is applied to the
154   Geostationary Operational Environmental Satellite (GOES-16) brightness temperature.

155   Figure 3 shows brightness temperature from the GOES-16 and moisture convergence, saturation
156   fraction, instability index and DCIN from the EC model averaged over all strong convective cases
157   (red line) and weak convective cases (black line) as a function of time. The vertical lines bound
158   the time of a day when OTREC dropsondes were deployed and assimilated into the EC model (12
159   to 18 UTC).

160   We see that the convection represented by moisture convergence peaks at 12 hours UTC, 0600
161   local time. This agrees with our observations while in the field. On average convection was
162   developing in the very early morning hours, becoming stratiform around 10 am local time, 16
163   UTC. The brightness temperature from satellite observations GOES-16 for the same cases has a
164   minimum that lags the maximum of the moisture convergence from the EC model. This is due to
165   a well-known lag between convection and resulting stratiform cloudiness as the upper troposphere
166   needs time to become optically thick (Bechtold et al., 2014). This gives us confidence in the
167   moisture convergence maximum at 12 UTC from the EC model. The second maximum in moisture
168   convergence that occurs at 20 UTC appears to be related to the overestimation of the diurnal
169   convection over nearby land. Note that spurious moisture convergence in EC at 20 UTC is not
170   supported by saturation fraction, instability index and DCIN values. The brightness temperature
171   does not support it either. Extensive research and comparison between satellite loops and the EC
172   model at 20 UTC show that frequently EC develops nonexistent convection in the B2 box. This is
173   known to the ECMWF and it was one of the reasons for their support of OTREC project and the
174   location of B2 box.
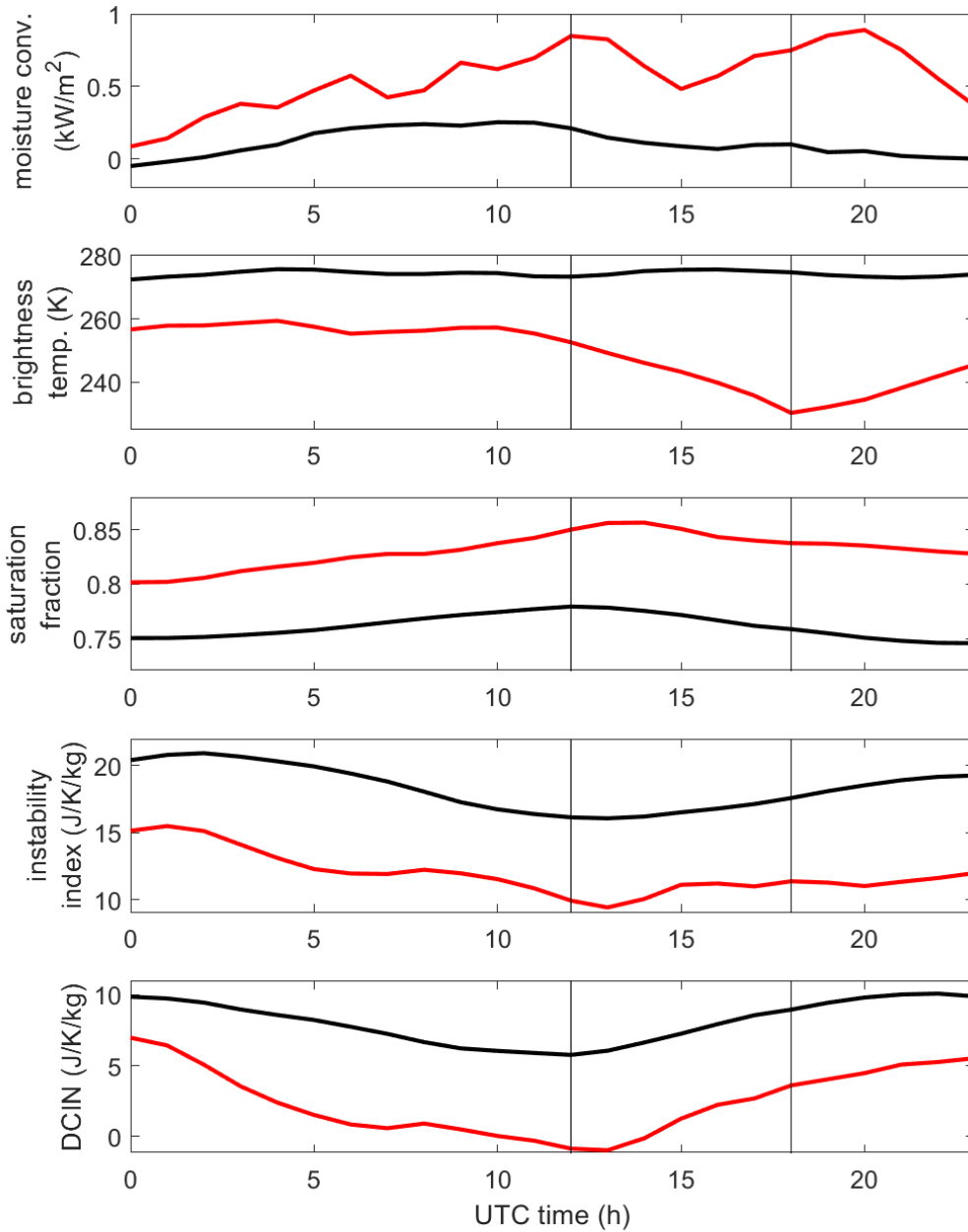
Figure 3: Moisture convergence from EC model, GOES-16 brightness temperature, saturation fraction, instability index and DCIN from EC model averaged over strong (red line) and weak (black line) convective cases from OTREC.

Prior to the peak in the moisture convergence at 12 UTC, we see that the saturation fraction increases. During that same time period the instability index and DCIN decrease. They reach their maximum (saturation fraction) and minima (instability index and DCIN) very close to the

maximum in moisture convergence. Our confidence in time evolution of saturation fraction, instability index and DCIN from the EC operational model is high as we have compared the EC model runs with and without dropsondes assimilated (not shown here). The agreement between the two is very good.

The weak time evolution represented by black line shows in contrast to convective line (in red) that moisture convergence is significantly less as is the saturation fraction. Instability index and DCIN have higher values.

3. Conclusions

The goal of this study is to study convection using data from two field projects, OTREC and PREDICT, and the ECMWF model.

Some of the questions that we try to answer are: Does physics of convection change with different SSTs and is it different if there is proximity to land? How does convection change when we go from strong to weak convection? Does the dependence on saturation fraction, instability index and DCIN change?

Vertically integrated moisture convergence is taken as a proxy for convection. This assumption is not ideal, but it is chosen to represent rainfall and therefore convection. Convection is classified into strong and weak categories. We look at the interplay of convection and thermodynamic parameters saturation fraction, instability index and DCIN for different phases of convection.

Strong convection looks very similar regardless to the environment, SST, proximity to land, different latitude etc. Saturation fraction shows anti-correlation with instability index and DCIN for every region that we have looked at. The fact that negative or small positive DCIN is needed for convection comes as no surprise (Raymond et al., 2003), while the instability index impact on convection has been less researched. We conclude that both, the boundary layer (DCIN) and free troposphere (saturation fraction and instability index) are very important for development of convection. As we move towards weak convection, the story becomes more complicated. The above correlations are less pronounced and more scattered.

The composite diurnal cycle of moisture convergence and thermodynamic parameters is analyzed using the ECMWF operational model for the events with strong and weak convection during OTREC. Before the peak of convection at 12 UTC saturation fraction increases and instability index and DCIN decrease. Maxima and minima of saturation fraction, instability index and DCIN are reached simultaneously. This further confirms the importance of thermodynamic parameters that not only correlate in OTREC and PREDICT scatter plots, but show in the time evolution that they are responsible for convection development.

It is important to note that we are looking at convection and the environment rather than the evolution of individual plumes. Such analysis gives broad statistical answers and could help improve cumulus parametrizations, Raymond and Fuchs-Stone (2020).

References

Arakawa, A. and W. H. Schubert, (1974), Interaction of a cumulus cloud ensemble with the large-scale environment, Part I. *J. Atmos. Sci.*, 31, 674-701.

Back, L. E., and C. S. Bretherton, (2009), On the relationship between SST gradients, boundary layer winds, and convergence over the tropical oceans, *J. Climate*, 33, 4182-4196.

Battisti, D. S., E. S. Sarachik, and A. C. Hirst, (1999), A consistent model for the large-scale steady surface atmospheric circulation in the tropics, *J. Climate*, 12, 2956-2964.

Bechtold, P., N. Semane, P. Lopez, J. Chaboureau, A. Beljaars, and N. Bormann, 2014: Representing Equilibrium and Nonequilibrium Convection in Large-Scale Models. *J. Atmos. Sci.*, **71**, 734–753, https://doi.org/10.1175/JAS-D-13-0163.1.

Fuchs, Ž. and Raymond, D. J, (2017), A simple model of intraseasonal oscillations, *J. Adv. Model. Earth Syst.*, 9, 1195– 1211, doi:10.1002/2017MS000963.

Fuchs-Stone, Z., D. J. Raymond and S. Sentic, (2020), OTREC2019: Convection over the East Pacific and Southwest Caribbean. *Geophys. Res. Lett.*, 47, doi:10.1029/2020GL087564.

Gjorgjievska, S. and D. J. Raymond, (2014), Interaction between dynamics and thermodynamics during tropical cyclogenesis, *Atmos. Chem. Phys.*, 14, 3065-3082.

Houze, R. A., (1989), Observed structure of mesoscale convective systems and implications for large-scale heating. *Quart. J. Roy. Meteor. Soc.*, 115, 425-461.

Houze, R. A., (2004), Mesoscale convective systems. *Rev. Geophys.*, 42, RG4003, doi:10.1029/2004RG000150.

Juracic, A., and D. J. Raymond, (2016), The effects of moist entropy and moisture budgets on tropical cyclone development. *J. Geophys. Res.*, 121, 9458-9473.

Lindzen, R. S., and S. Nigam, (1987), On the role of sea surface temperature gradients in forcing low-level winds and convergence in the tropics, *J. Atmos. Sci.*, 44, 2418-2436.

259 Lopez Carrillo, C., and D. J. Raymond, (2011), Retrieval of three-dimensional wind fields from
260 Doppler radar data using an efficient two-step approach. *Atmos. Meas. Tech.*, 4, 2717-2733,
261 doi:10.5194/amt-4-2717-2011.

262 Montgomery, M. T., Davis, C., Dunkerton, T., Wang, Z., Velden, C., Torn, R., Majumdar, S. J.,
263 Zhang, F., Smith, R. K., Bosart, L., Bell, M. M., Haase, J. S., Heymsfield, A., Jensen, J., Campos,
264 T., and Boothe, M. A., (2012), The Pre-Depression Investigation of Cloudsystems in the Tropics
265 (PREDICT) experiment, *B. Am. Meteor. Soc.*, 93, 153–172.

266 Palmen, E. H., (1948), On the Formation and Structure of Tropical Cyclones," *Geophysica,*
267 *Helsinki*, Vol. 3, pp. 26-38.

268 Raymond, D. J., G. B. Raga, C. S. Bretherton, J. Molinari, C. Lopez-Carrillo, and Z. Fuchs, (2003),
269 Convective forcing in the intertropical convergence zone of the eastern Pacific, *J. Atmos. Sci.*, 60,
270 2064-2082.

271 Raymond, D. J., S. L. Sessions, and C. Lopez Carrillo, (2011), Thermodynamics of tropical
272 cyclogenesis in the northwest Pacific, *J. Geophys. Res.*, 116, D18101,
273 doi:10.1029/2011JD015624.

274 Raymond, D. J. and C. Lopez Carrillo, (2011), The vorticity budget of developing typhoon Nuri
275 (2008), *Atmos. Chem. Phys.*, 11, 147-163, doi:10.5194/acp-11-147-2011.

276 Raymond, D. J., S. Gjorgjievska, S. Sessions, and Z. Fuchs, (2014), Tropical cyclogenesis and
277 mid-level vorticity. *Australian Meteorological and Oceanographic Journal*, 64, 11-25.
278
279 Raymond, D. J., Z. Fuchs, S. Gjorgjievska and S. L. Sessions, (2015), Balanced dynamics and
280 convection in the tropical troposphere. *J. Adv. Model. Earth Syst.*, 7, doi:10.1002/2015MS000467.
281
282 Raymond, D. J. and M. M. Flores, (2016), Predicting convective rainfall over tropical oceans from
283 environmental conditions. *J. Adv. Model. Earth Syst.*, 8, doi:10.1002/2015MS000595.
284
285 Raymond, D. J., (2017), Convection in the east Pacific intertropical convergence zone. *Geophys.*
286 *Res. Lett.*, 44, 562-568, doi:10.1002/2016GL071554.
287
288 Raymond, D. J. and G. Kilroy, (2019), Control of convection in high-resolution simulations of
289 tropical cyclogenesis. *J. Adv. Model. Earth Syst.*, 11, 1582-1599.
290
291 Raymond and Fuchs-Stone, (2020), Emergent Properties of Convection in OTREC and PREDICT.
292 *Journal of Geophysical Research: Atmospheres.* In press.
293
294 Riehl, H., T. C. Yeh, J. S. Malkus and N. E, La Seur, (1951), The north-east trade of the Pacific
295 ocean, *Quart. J. Roy. Meteor. Soc.*, 77, 598-626.

296 Sentić, S., Sessions, S. L., and Fuchs, Ž., (2015), Diagnosing DYNAMO convection with weak
297 temperature gradient simulations, *J. Adv. Model. Earth Syst.*, 7, 1849– 1871,
298 doi:10.1002/2015MS000531.

299   Sentić, S., Fuchs-Stone, Ž., & Raymond, D. J, (2020), The Madden-Julian Oscillation and mean
300   easterly winds. *Journal of Geophysical Research: Atmospheres*, 125,
301   e2019JD030869. https://doi.org/10.1029/2019JD030869

302   Singh, M. S., Warren, R. A., & Jakob, C., (2019), A steady-state model for the relationship
303   between humidity, instability, and precipitation in the tropics. *Journal of Advances in Modeling*
304   *Earth Systems*, **11**, 3973– 3994. https://doi.org/10.1029/2019MS001686

305   Stevens, B., J. Duan, J. C. McWilliams, M. Munnich, and J. D. Neelin, (2002), Entrainment,
306   Rayleigh friction, and boundary layer winds over the tropical Pacific, *J. Climate*, 15, 30-44.

307   Tomas, R. A., J. R. Holton, and P. J. Webster, (1999), The influence of cross-equatorial pressure
308   gradients on the location of near-equatorial convection, *Quart. J. Roy. Meteor. Soc.*, 125, 1107-
309   1127.

310   UCAR/NCAR - Earth Observing Laboratory, Voemel, H. 2019. NCAR/EOL AVAPS Dropsonde
311   QC   Data.   Version   1.0.   UCAR/NCAR   -   Earth   Observing
312   Laboratory. https://doi.org/10.26023/EHRT-TN96-9W04. Accessed 13 January 2020.

313   Yu, L., Jin, X., & Weller, R. A, (2008), Multidecade global flux datasets from the Objectively
314   Analyzed Air-sea Fluxes (OAFlux) Project: Latent and sensible heat fluxes, ocean evaporation,
315   and related surface meteorological variables. Woods Hole Oceanographic Institution, OAFlux
316   Project Technical Report. OA-2008-01, 64pp. Woods Hole, Massachusetts, USA.

317   Zipser, E. J., (1969), The role of organized unsaturated convective downdrafts in the structure and
318   rapid decay of an equatorial disturbance. *J. Appl. Meteor.*, 8, 799-814.

319   Zipser, E. J., (1977), Mesoscale and convective scale downdrafts as distinct components of squall-
320   line structure. *Mon. Wea. Rev.*, 105, 1568-1589.